

Cftr controls lumen expansion and function of Kupffer's vesicle in zebrafish

Adam Navis, Lindsay Marjoram and Michel Bagnat*

SUMMARY

Regulated fluid secretion is crucial for the function of most organs. In vertebrates, the chloride channel cystic fibrosis transmembrane conductance regulator (CFTR) is a master regulator of fluid secretion. Although the biophysical properties of CFTR have been well characterized *in vitro*, little is known about its *in vivo* role during development. Here, we investigated the function of Cftr during zebrafish development by generating several *cftr* mutant alleles using TAL effector nucleases. We found that loss of *cftr* function leads to organ laterality defects. In zebrafish, left-right (LR) asymmetry requires cilia-driven fluid flow within the lumen of Kupffer's vesicle (KV). Using live imaging we found that KV morphogenesis is disrupted in *cftr* mutants. Loss of Cftr-mediated fluid secretion impairs KV lumen expansion leading to defects in organ laterality. Using bacterial artificial chromosome recombineering, we generated transgenic fish expressing functional Cftr fusion proteins with fluorescent tags under the control of the *cftr* promoter. The transgenes completely rescued the *cftr* mutant phenotype. Live imaging of these transgenic lines showed that Cftr is localized to the apical membrane of the epithelial cells in KV during lumen formation. Pharmacological stimulation of Cftr-dependent fluid secretion led to an expansion of the KV lumen. Conversely, inhibition of ion gradient formation impaired KV lumen inflation. Interestingly, cilia formation and motility in KV were not affected, suggesting that fluid secretion and flow are independently controlled in KV. These findings uncover a new role for *cftr* in KV morphogenesis and function during zebrafish development.

KEY WORDS: Cftr, Fluid secretion, Kupffer's vesicle, Zebrafish

INTRODUCTION

Regulated fluid secretion is crucial for the development and function of many organs in vertebrates, including the kidney, vasculature, brain and ear (Cartwright et al., 2009). During organogenesis, fluid secretion can act as a force driving tubulogenesis. In zebrafish, fluid secretion promotes single lumen formation in the gut (Bagnat et al., 2007) and ventricle inflation in the brain (Lowery and Sive, 2005). Similarly, in mammals, fluid secretion has been shown to be crucial for lung development (Wilson et al., 2007). Loss of fluid regulation can lead to defects in organogenesis. For example, excessive fluid accumulation leads to dramatic expansion of the zebrafish gut lumen (Bagnat et al., 2010) and defects in cilia-dependent fluid clearance can lead to kidney cysts and hydrocephalus (Kramer-Zucker et al., 2005; Moyer et al., 1994; Nauli et al., 2003; Sun et al., 2004).

A major regulator of fluid secretion in vertebrates is the chloride channel cystic fibrosis transmembrane conductance regulator (CFTR). CFTR regulates fluid secretion by controlling the transport of chloride (Anderson et al., 1991), which draws sodium to generate osmotic gradients that drive the movement of water through a tissue. Defects in CFTR function cause cystic fibrosis (CF), a disease in which loss of Cl⁻ and/or HCO₃⁻ transport impairs fluid secretion and also causes mucus build-up in many organs, including the lungs, intestine and pancreas (Durie and Forstner, 1989; Gaskin et al., 1988; Matsui et al., 1998). The channel is composed of several domains, including twelve transmembrane domains, two nucleotide-binding domains and a unique regulatory domain (R-

domain) (Riordan et al., 1989). The R-domain is regulated through phosphorylation by cyclic AMP-dependent protein kinase (PKA) (Berger et al., 1993). Zebrafish Cftr is highly similar to its human ortholog, particularly in domains important for CFTR function (Bagnat et al., 2010). Although CFTR activity has been well characterized *in vitro*, relatively little is known about its function *in vivo*, especially during development.

In vertebrates, fluid flow generated by ciliary beating is important for the determination of left-right (LR) asymmetry. In zebrafish, laterality is controlled by a transient, fluid-filled structure called Kupffer's vesicle (KV) (Essner et al., 2005). KV is functionally homologous to the organs of asymmetry in other vertebrates, including the mouse node and the gastrocoel roof plate in *Xenopus* (Nonaka et al., 2002; Schweickert et al., 2007). KV develops from a group of dorsal forerunner cells (DFCs) that migrate to the vegetal pole during gastrulation and coalesce to form a fluid-filled spherical structure surrounding a single lumen (Amack et al., 2007; Oteiza et al., 2008). Within the KV lumen, motile cilia drive directional fluid flow leading to asymmetric calcium signaling at the periphery, similar to the mouse node (McGrath et al., 2003; Sarmah et al., 2005). Asymmetric signaling leads to an upregulation of left-sided genes beginning with *southpaw* (*spaw*), the zebrafish ortholog of Nodal, a highly conserved signaling molecule required for the specification of LR asymmetry (Brennan et al., 2002; Long et al., 2003; Saijoh et al., 2003). Although it has been well established that cilia-driven fluid flow is crucial for KV function, the mechanisms that regulate secretion of fluid into KV remain uncharacterized.

Here, we describe a new role for Cftr in the development and function of KV in zebrafish. Using TAL effector nucleases (TALENs), we generated *cftr* mutants and found that loss of Cftr activity impairs KV lumen expansion and function, causing defects in LR patterning. Using bacterial artificial chromosome (BAC) recombineering we generated a Cftr-GFP transgenic line and

Department of Cell Biology, Duke University Medical Center, Durham, NC 27710, USA.

* Author for correspondence (m.bagnat@cellbio.duke.edu)

observed that *cfr* is expressed primarily in KV, where the protein localizes apically as the lumen forms. Together, our results demonstrate that Cfr-dependent fluid secretion is crucial for lumen formation and function of KV in zebrafish.

MATERIALS AND METHODS

Fish stocks

Zebrafish were maintained at 28°C and propagated as previously described (Westerfield, 2000). The following zebrafish lines were used for this work: AB, EK, *Tg(sox17:GFP)s870* (Sakaguchi et al., 2006), *Tg(fabp10:dsRed, ela:GFP)gz12* (Farooq et al., 2008), *TgBAC(cfr-GFP)pd1041*, *TgBAC(cfr-RFP)pd1042*, *cfr^{pd1048}*, *cfr^{pd1049}*, *cfr^{pd1050}* and *Tg(hsp70l:GFP-podxl)pd1080* (this study).

TALEN-mediated mutagenesis

Three TALENs (Miller et al., 2011) were designed to target the sixth exon of *cfr* using TALEN targeter (Doyle et al., 2012) and constructed using Golden Gate assembly (Cermak et al., 2011). The TALEN used to generate the *cfr* mutant alleles reported here was composed of the following TAL effector domains: NN NN NN NG NI NG NN NN HD HD HD NI NG NG NG NG NI NG NI NG and NN NG NI HD NI HD NI NN NN NI NG NN HD NI NG NG. Zebrafish were injected into the yolk at the one-cell stage with 100 pg total TALEN RNA and 50 pg of dsRed RNA to mark expressing embryos. Mutant alleles were identified by *EcoRV* digestion of a PCR product generated with the following primers: *cfr*-exon6-F, TTGGCCTAAATTCAAATGAT; and *cfr*-exon6-R, TTTGGATGC-ACAGTAGGCTAA.

BAC recombineering and transgenesis

A BAC containing *cfr* (DKEY-270I2) was modified using Red/ET BAC modification plasmids (GeneBridges, Heidelberg, Germany). A positive selection cassette for generating C-terminal fusions was developed by constructing a plasmid containing a 20-aa spacer (DLPAEQKLISEEDLDPPVAT), GFP or mRFP-Ruby, an SV40 polyadenylation sequence, and an FRT-kanamycin-FRT cassette (Lee et al., 2001) into pBluescript. Recombination was performed by amplifying the cassette with the following primers, which contained 50 bp of homology flanking the stop codon: *cfr*-spGFP-hom-F, CGCAGACCCTGCAAGAGGAGG-CAGAGACAACATCCAGGACACTCGCTCGATCTCCCCGCCGAA-CAGAAA and *cfr*-spGFP-hom-R, TTTAATGTACCATTGGGTGACG-GCCTGGGTCACTGAGTCTTTTGGAAACGCATTGGAGTCCACCGC-GGTG. The amplicon was then transformed into Red/ET-induced *Escherichia coli*. The kanamycin was removed from the BAC by expressing FIpase from the p707-FIpe plasmid (GeneBridges). The *cfr*-RFP BAC was further modified by recombining the iTo2-Amp cassette into the loxP site of the pIndigoBAC-536 backbone (Suster et al., 2009). The modified BAC was purified using the Nucleobond BAC-100 Kit (Clontech, Mountain View, CA, USA). The *cfr*-GFP BAC was linearized using *SfiI* (NEB) and injected into one-cell-stage embryos. The *cfr*-RFP BAC was co-injected with 50 pg of transposase into one-cell-stage embryos (Kawakami, 2004; Kwan et al., 2007). Two transgenic lines were established: *TgBAC(cfr-GFP)pd1041* and *TgBAC(cfr-RFP)pd1042*.

The *Tg(hsp70l:GFP-podxl)pd1080* line was generated by Gateway recombination with the Tol2Kit (Kwan et al., 2007). GFP-podocalyxin (Meder et al., 2005) was subcloned into pME and assembled with p5E-hsp70l, p3E-polyA and pDestTol2pA2. The resulting plasmid was co-injected into one-cell-stage embryos with 50 pg Transposase RNA. To induce expression, embryos at 50% epiboly were heat-shocked for 30 minutes in a 39°C water bath. GFP-podocalyxin was imaged in conjunction with GFP Counterstain BODIPY TR Methyl Ester dye (Invitrogen).

In situ hybridization

The probe to detect the *cfr* transcript by *in situ* hybridization was PCR amplified from cDNA and ligated into pGEMT-Easy (Promega, Madison, WI, USA) with the following primers: *cfr*-ish-F, CCAAACCAGACAA-AGGCAAA; and *cfr*-ish-R, GGTGCCATCTCACGATAACTCAA. *In situ* hybridization was performed as previously described (Marjoram and Wright, 2011; Snelson et al., 2008). Detection of *spaw*, *cmlc2* (*myl7* –

Zebrafish Information Network), *lefty1* and *no tail* transcripts were performed as previously described (Long et al., 2003; Yelon et al., 1999). The plasmids were linearized and digoxigenin-labeled RNA was generated using the DIG RNA Labeling Kit (Roche). Stained embryos were imaged on a Discovery.V20 stereoscope (Zeiss, Oberkochen, Germany) with an Achromat S 1.0× lens.

Immunofluorescence

Whole-mount immunofluorescence using aPKC (Santa Cruz Biotechnology; 1/100), pan-cadherin (Santa Cruz Biotechnology; 1/1200) and ZO-1 (Invitrogen; 1/500) primary antibodies with goat anti-mouse Alexa568 or goat anti-rabbit Alexa647 secondary antibodies (Molecular Probes; 1/100) was performed as previously described (Li et al., 2011). Acetylated tubulin staining was performed as previously described (Zaghloul and Katsanis, 2011) with the following modifications. Embryos were fixed overnight at 4°C in Dent's fixative, treated with 10 µg/ml Proteinase K (Sigma) for 1 minute and post-fixed with 4% paraformaldehyde. Mouse anti-acetylated tubulin (Sigma; 1/1000) was detected with goat anti-mouse Alexa568 (Molecular Probes; 1/100). Tailbuds were dissected with a microknife (Fine Science Tools, Foster City, CA, USA), mounted in SlowFade Gold (Invitrogen) and imaged using a Leica SP5 confocal microscope.

KV live imaging

Embryos for live confocal imaging were mounted in 4% agarose on slides and immediately imaged on an SP5 confocal microscope (Leica, Wetzlar, Germany) with an HC PL APO 20×/0.70 objective. Imaging of KV flow was performed by injecting fluorescent beads as previously described (Borovina et al., 2010). Differential interference contrast (DIC) microscopy and whole-mount epifluorescence were performed on embryos mounted in 3% methylcellulose and imaged on an Imager M1 (Zeiss) with a EC Plan-Neofluar 10×/0.3 objective.

RNA injection

The *TgBAC(cfr-GFP)* open reading frame was cloned into pCS2+ with flanking *EcoRI* sites. RFP was fused to the N-terminus of Clc5b (accession number: BC085448) and cloned into pCS2+ with flanking *EcoRI* and *XhoI* sites. Capped RNA was transcribed from *NotI* linearized plasmid using the mMESSAGE mMACHINE SP6 Kit (Ambion, Grand Island, NY, USA). *cfr*-GFP (150 pg/embryo) or Arl13b-mCherry (75 pg/embryo) (Borovina et al., 2010) RNA was injected into the yolk of one-cell-stage embryos.

Pharmacological treatments

Pharmacological reagents were purchased from Sigma (St Louis, MO, USA). Forskolin was prepared as a 10 mM stock in DMSO and fish were treated in egg water at 10 µM. IBMX (3-isobutyl-1-methylxanthine) was prepared as a 100 mM stock in DMSO and embryos were treated at 40 µM in egg water. Ouabain was prepared as a 1 mM stock in DMSO and embryos were treated at 1 µM in egg water. Embryos were treated from 50% epiboly until they were imaged at the 10- to 12-somite stage (ss).

Cell culture

Human HEK293 and Cos-7 cells were cultured in DMEM with 10% fetal bovine serum and 1% penicillin-streptomycin (Invitrogen). Cells were transfected on glass coverslips with either pCDNA-Cfr-GFP or pCDNA-Cfr^{pd1048}-GFP using Lipofectamine 2000 (Invitrogen) and fixed the following day in 4% paraformaldehyde. Fixed cells were stained with DAPI and imaged on an Imager M1 (Zeiss).

Statistical analysis

Measurements of KV lumen area and cilia length were performed using ImageJ (NIH, Bethesda, MD, USA) and analyzed for statistical significance using Student's *t*-test in Prism (Graphpad, La Jolla, CA, USA). Comparisons between KV phenotype and organ laterality were performed using a χ^2 test in Prism (Graphpad).

RESULTS

Generation of zebrafish *cfr* mutants

To investigate the role of Cfr during zebrafish development we generated *cfr* mutants using TALENs (Cermak et al., 2011; Huang

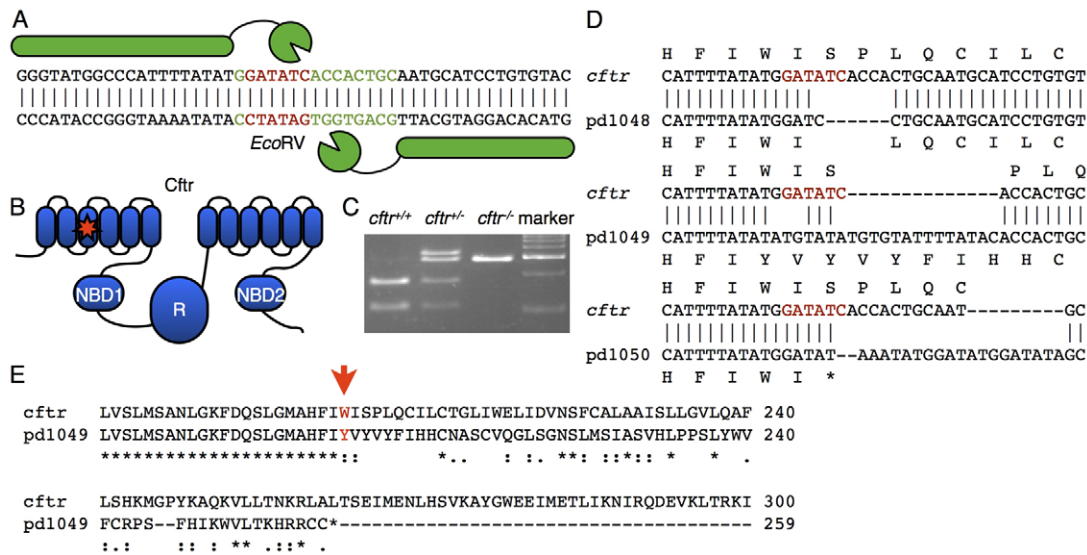


Fig. 1. Generation of a *cftr* mutant zebrafish. (A) A TALEN was designed to target the *EcoRV* site in the sixth transmembrane domain. The spacer is marked by green text and the restriction site is denoted by red text. (B) Schematic of the domain structure of Cftr with a star indicating the TALEN target site within the third transmembrane domain of the protein. NBD, nucleotide binding domain; R, regulatory domain. (C) TALEN activity generated insertions and deletions that disrupt the *EcoRV* site. (D) Sequence alignments of the TALEN-generated alleles. *Cftr*^{pd1048} has a six-nucleotide deletion, *cftr*^{pd1049} and *cftr*^{pd1050} have nucleotide insertions and deletions causing frameshifts leading to premature stop codons. (E) An alignment of the amino acid sequences encoded by *cftr*^{pd1049} and WT *cftr*.

et al., 2011; Miller et al., 2011). Three TALEN pairs for *cftr* were constructed, transiently expressed in zebrafish embryos and then screened for activity. Embryos injected with the TALEN pair showing the highest transient activity were raised to establish mutant lines. The TALEN was targeted to the *EcoRV* site in the sixth of 27 *cftr* exons, corresponding to the third transmembrane domain. This exon precedes several domains crucial for Cftr function, including the chloride pore, regulatory domain and both nucleotide-binding domains (Fig. 1A,B). After screening ten TALEN-injected fish for disruption of the *EcoRV* restriction site (Fig. 1C), we identified three *cftr* alleles, including a two-amino acid deletion, *cftr*^{pd1048}, and two frameshift mutations, *cftr*^{pd1049} and *cftr*^{pd1050} (Fig. 1D). The *cftr*^{pd1049} allele is predicted to code for 56 incorrect amino acids past the lesion before encountering a stop codon (Fig. 1E), whereas *cftr*^{pd1050} generates a stop codon at the site of the lesion. To characterize the *cftr*^{pd1048} mutation, we cloned and expressed GFP-tagged wild-type (WT) Cftr (Cftr-GFP) and Cftr^{pd1048}-GFP in Cos-7 cells. Unlike WT Cftr-GFP, Cftr^{pd1048}-GFP was largely absent at the cell surface and localized mostly to intracellular membranes resembling the endoplasmic reticulum, suggesting that the shortened transmembrane domain encoded by the mutant allele affects biosynthetic transport (supplementary material Fig. S1A,B). Accordingly, in transfected cells Cftr^{pd1048} lacked the mature, fully glycosylated form of the protein, as judged by western blot analysis (supplementary material Fig. S1C).

***cftr* is required for the specification of left-right asymmetry**

To analyze Cftr function during development, the *cftr* mutations were crossed into the *Tg(fabp10:dsRed, ela:GFP)gz12* background, which expresses dsRed in the liver and GFP in the exocrine pancreas (Farooq et al., 2008). While examining homozygous mutant embryos, we found inversion of liver and pancreas situs. In zebrafish, the liver normally develops on the left side of the abdomen; however, in 27% of *cftr*^{pd1049} mutants the liver developed

on the right ($n=30$ mutants), compared with 0% of their WT siblings ($n=103$ WT) (Fig. 2A,B).

To test whether the anatomical positioning of other organs is also affected in *cftr* mutants, we examined heart looping, one of the earliest morphological indicators of organ laterality. The heart, marked by *cmhc2* expression, normally loops to the left. In ~31% of *cftr* mutant embryos the heart looped to the right ($n=138$ mutants), in contrast to only 1% of WT siblings ($n=408$ WT) (Fig. 2C,D). Homozygous mutants survived to adulthood and the females were moderately fertile, allowing the generation of maternal zygotic *cftr*^{pd1049} mutants. Maternal zygotic *cftr*^{pd1049} fish were morphologically identical to zygotic *cftr*^{pd1049} and had similar rates of reversed heart looping (31%, $n=26$). Defects in liver and heart orientation were primarily concordant and only a few cases of heterotaxia were observed.

To investigate early events in LR patterning, we examined the expression of *spaw*, a gene asymmetrically expressed in the left lateral plate mesoderm of the embryo at 20 ss and an important LR patterning determinant (Long et al., 2003). Whereas 99.3% of WT siblings expressed *spaw* exclusively on the left ($n=146$), *cftr*^{pd1049} mutants displayed a range of *spaw* expression phenotypes including exclusively left (30.6%), left dominant (25.0%), bilateral (23.6%), right dominant (9.7%) and exclusively right (11.1%) ($n=73$) (Fig. 2E,F). These data indicate that *cftr* is required for the establishment of LR asymmetry in zebrafish before the onset of *spaw* expression.

Aberrant *spaw* expression and organ laterality can be caused by defects in processes that establish and restrict asymmetric signaling. Dorsal midline structures, such as the notochord and floorplate, function as a barrier to restrict *spaw* to the left side of the embryo and loss of barrier function has been shown to result in bilateral *spaw* expression (Long et al., 2003). Additionally, midline expression of *lefty1*, a *spaw* antagonist, is required for left-sided restriction of *spaw* expression (Bisgrove et al., 1999). To determine whether *cftr*^{pd1049} mutants have midline barrier defects, we

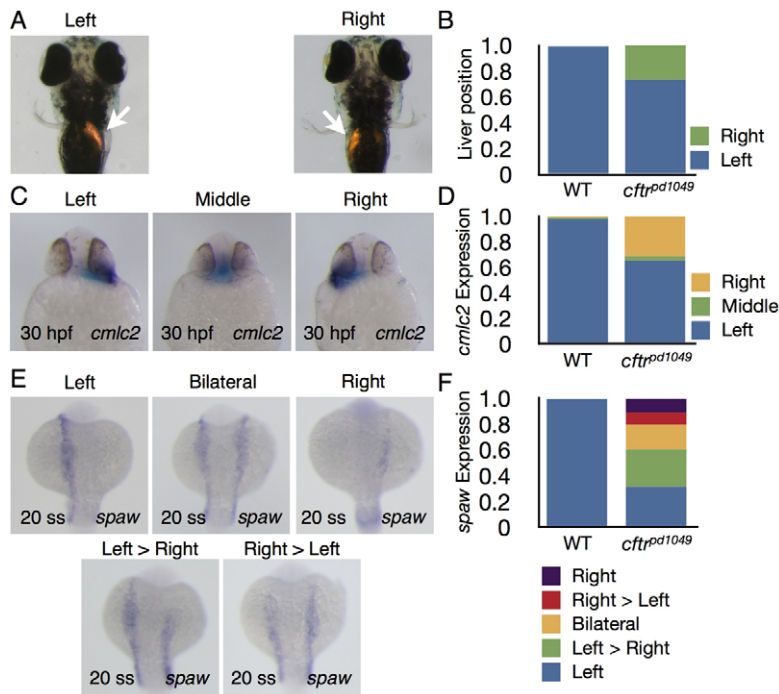


Fig. 2. Organ laterality is disrupted in *cftr*¹⁰⁴⁹ mutant embryos. Heterozygous *cftr*^{pd1049} fish were mated to assess organ laterality. (A) Ventral view of 4 days post-fertilization (dpf) WT and *cftr*^{pd1049} mutant larvae expressing dsRed in the liver (arrows). (B) Quantification of liver orientation in WT and *cftr*^{pd1049} mutants. Liver orientation is reversed in 27% of homozygous mutants. WT, *n*=103; *cftr*^{pd1049}, *n*=30. (C) Ventral view of representative *cftr*^{pd1049} mutants showing *cmc2* expression pattern. (D) Quantification of heart looping in WT and *cftr*^{pd1049} mutants. WT, *n*=408; *cftr*^{pd1049}, *n*=138. (E) Dorsal view of *cftr*^{pd1049} mutant embryos displaying left, right, left>right, right>left and left=right *spaw* expression patterns. (F) Quantification of *spaw* expression in WT and *cftr*^{pd1049} mutants. WT, *n*=146; *cftr*^{pd1049}, *n*=73.

examined the expression of midline markers as well as the gross morphology of WT and mutant embryos. At 22 ss, expression of the notochord marker *no tail* (*ntl*) in *cftr*^{pd1049} mutants was indistinguishable from that of WT siblings (supplementary material Fig. S2A,B). We also examined the expression of *lefty1* and found that in *cftr*^{pd1049} mutant embryos *lefty1* expression was similar to that of WT siblings (supplementary material Fig. S2C,D). In addition, the notochord and floorplate of *cftr*^{pd1049} mutants appeared to be completely intact at 24 hours post-fertilization (hpf) as judged by DIC microscopy (supplementary material Fig. S2E,F). Brightfield whole-mount imaging of *cftr*^{pd1049} mutants at 24 and 48 hpf showed no obvious morphological defects (supplementary material Fig. S2G-J). Thus, defects in *spaw* expression and LR patterning in *cftr*^{pd1049} mutants are probably not due to defects in midline integrity.

Lumen expansion in KV requires *cftr*

To understand better how Cfr functions in LR asymmetry, we next investigated the development of KV, a transient, fluid-filled organ important for the specification of LR asymmetry in zebrafish (Essner et al., 2005). Examination of *cftr* mutants by DIC microscopy revealed that the KV lumen was absent in the frameshift alleles *cftr*^{pd1049} and *cftr*^{pd1050} (Fig. 3A-D). This phenotype is fully penetrant; all homozygous *cftr* mutants displayed defects in KV lumen morphogenesis (*n*=72). In *cftr*^{pd1048}, the lumen was present, but severely reduced in size (Fig. 3E,F), suggesting that this may be a hypomorphic allele.

To investigate the morphology of KV in greater detail, we crossed *cftr* mutants into the *Tg(sox17:GFP)s870* background, a well-established marker of DFCs and KV (Oteiza et al., 2008; Sakaguchi et al., 2006). To visualize cilia, we injected RNA encoding Arl13b-mCherry into one-cell-stage embryos (Borovina et al., 2010). Using live confocal imaging, we found that in *cftr*^{pd1049} mutants the DFCs migrated and clustered to form a structure similar in size to the WT KV. However, in the mutants, lumen inflation did not occur and resulted in a central plate of ciliated, *sox17:GFP*-positive cells with no discernible luminal space (Fig. 3G,H).

Next, we examined KV development in the hypomorphic *cftr*^{pd1048} allele. Using live confocal imaging we observed that, at 10 ss, mutants homozygous for this allele had a KV with a very small central lumen (~30% of the area compared with WT siblings) containing Arl13b-mCherry-positive cilia that appeared motile (Fig. 3L,J). Owing to line averaging during confocal microscopy, motile cilia appear as a fan-shaped blur (Borovina et al., 2010). At 12 ss, in some rare cases, the small lumen inflated to a size large enough to reveal seemingly normal, but highly crowded motile cilia (supplementary material Fig. S3A-D), suggesting that Cfr function is not required for cilia morphogenesis or motility in KV. We then investigated whether these mutants formed a lumen large enough to allow for proper specification of LR asymmetry. We examined heart looping and liver orientation in *cftr*^{pd1048} mutants and found that they had a similar rate of LR asymmetry defects compared to the null (*cftr*^{pd1049}) allele (data not shown). To determine whether fluid flow is normal in the hypomorphic allele, we injected fluorescent beads into the KV lumen. In the *cftr*^{pd1048} KV, fluid flow appeared turbulent, indicating the organ does not function normally when fluid secretion and lumen size are significantly reduced (supplementary material Fig. S3E,F).

To examine KV ciliogenesis further in the absence of Cfr function and lumen expansion, we determined the number and average length of cilia in KV. We found no significant difference in either the number or length of cilia between *cftr*^{pd1049} mutants and their WT siblings (Fig. 3K-N), indicating that the volume of the KV lumen does not regulate ciliogenesis.

We next examined the apical-basal polarity of KV in *cftr*^{pd1049} mutants, by investigating the localization of several polarity markers. We characterized membrane polarity by examining the localization of the tight-junction protein ZO-1 and the basolateral marker, Cadherin. In mutant embryos, ZO-1 and Cadherin were properly localized in the absence of lumen expansion (Fig. 4A,B). A higher magnification view of the KV epithelium shows that ZO-1 appears completely apical and Cadherin is absent from the apical membrane in WT and *cftr*^{pd1049} mutant embryos (Fig. 4A'-B'). We next examined aPKC, a peripheral membrane protein localized to

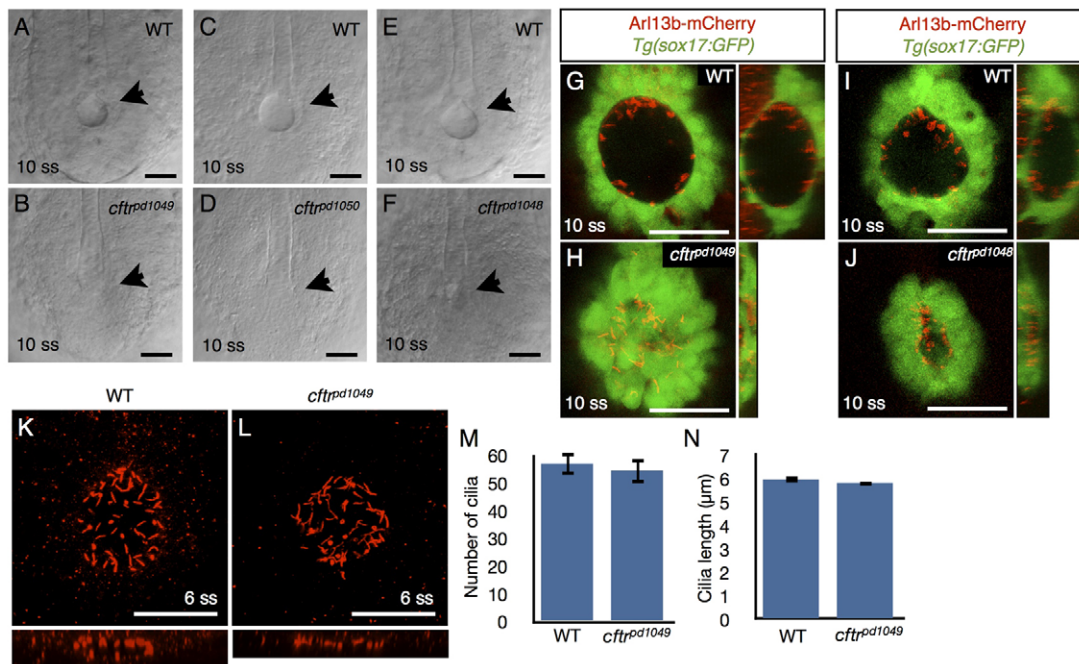


Fig. 3. KV lumen inflation requires *cftr*. (A–F) KV lumen (arrow), imaged at 10 ss by DIC microscopy in WT (A,C,E) and mutant siblings (B,D,F) respectively. (B,D) The KV lumen is undetectable by DIC in *cftr^{pd1049}* and *cftr^{pd1050}* mutants at 10 ss. (F) DIC imaging of the *cftr^{pd1048}* tailbud identified a small KV lumen. (G–J) Live confocal images showing ventral cross-section and orthogonal views of WT and mutant KV expressing *Tg(sox17:GFP)* and *Arl13b-mCherry* RNA at 10 ss in (G,H) WT and *cftr^{pd1049}* mutant siblings and (I,J) WT and *cftr^{pd1048}* siblings. (K,L) Confocal images of WT and mutant KV stained for acetylated tubulin. (M) Quantification of the number of KV cilia. WT KV contained 57.0 ± 4.1 cilia ($n=5$) and mutant KV contained 54.5 ± 4.6 cilia ($n=8$) ($P=0.69$). (N) Quantification of cilia length in WT and mutant KV. WT cilia length was 5.97 ± 0.13 μm ($n=30$) and *cftr^{pd1049}* cilia length was 5.82 ± 0.13 μm ($n=49$) ($P=0.42$). Error bars represent s.e.m. Scale bars: 50 μm .

the apical membrane in KV (Amack et al., 2007). In *cftr^{pd1049}* mutants, we observed a plate of aPKC-positive membrane on the center (apical side) of the *sox17:GFP*-positive cluster (Fig. 4C,D). We also generated a transgenic line expressing an integral membrane apical marker, *GFP-podocalyxin* (*GFP-podxl*) (Meder et al., 2005) under the control of a heat shock promoter. We observed that in *cftr^{pd1049}* mutants, at 3 ss, *GFP-podxl* was also localized in a central plate of apical membrane in KV (Fig. 4E,F). To observe the morphology of the KV lumen in *cftr^{pd1049}* mutants better, we live-imaged the localization of an apical peripheral membrane protein, RFP-Clic5b, in *Tg(sox17:GFP)*-expressing embryos. Injection of *RFP-clic5b* RNA marked the apical membrane in WT and *cftr^{pd1049}* mutant KV (Fig. 4G,H). Thus, apical-basal polarity in the KV epithelium develops properly in *cftr* mutants. Altogether, these data indicate that *cftr* is crucial for lumen expansion but not ciliogenesis or apical-basal polarization during KV morphogenesis.

Cftr is expressed and apically localized in KV

To determine where *Cftr* functions during KV lumen formation, we examined *cftr* expression using *in situ* hybridization and live imaging. By *in situ* hybridization, *cftr* expression was highly enriched in KV at 3 ss, a stage when the lumen is expanding (Fig. 5A). By 10 ss, the transcript appeared to be downregulated and *cftr* expression was also observed in the chordamesoderm (Fig. 5B).

To understand the dynamics of *Cftr* expression and localization better in live embryos, we used recombineering to generate a *Cftr*-GFP fusion protein. The *cftr* BAC (DKEY-27012) used contains ~50 kb of genomic DNA upstream and 100 kb downstream of the coding

sequence, and is likely to include critical regulatory information (Fig. 5C). To generate a C-terminal fusion protein, we replaced the stop codon of *cftr* with GFP, separated by a sequence encoding a 20 amino acid spacer to provide some insulation from GFP. C-terminal fusion proteins of human CFTR maintain similar localization and channel activity to untagged CFTR (Benharouga et al., 2003). We then repeated the recombineering procedure to generate an RFP fusion and established two transgenic lines, *TgBAC(cftr-GFP)pd1041* and *TgBAC(cftr-RFP)pd1042*, that have identical expression patterns at all stages observed. At 10 ss, by whole-mount epifluorescence, *Cftr*-GFP was highly restricted to KV (Fig. 5D-G). Next, we performed live, time-lapse imaging of *TgBAC(cftr-RFP)* in conjunction with cytosolic *Tg(sox17:GFP)* and found that *Cftr*-RFP was localized apically in KV by 1 ss and throughout the initial stages of lumen formation as multiple small lumens coalesced into a single lumen (Fig. 6A,B; supplementary material Movie 1). By 10 ss, *Cftr*-RFP remained apically localized as the lumen continued to expand (Fig. 6C,D). At 15 ss, prior to KV disassembly, *Cftr*-GFP expressed from *TgBAC(cftr-GFP)* remained localized to the apical membrane (Fig. 6E,F). Together, these data indicate that *Cftr* is expressed and apically localized in KV throughout its morphogenesis.

Regulated fluid secretion requires *Cftr* in KV

Next, we tested whether modulation of *Cftr* channel activity could regulate the luminal volume of KV. *Cftr* is strongly activated by phosphorylation of its R-domain by PKA (Berger et al., 1993). To activate *Cftr*, we treated fish with a cocktail of forskolin and IBMX. These drugs synergistically elevate cAMP levels, rapidly increasing PKA activity, and result in a potent activation of *Cftr*. PKA

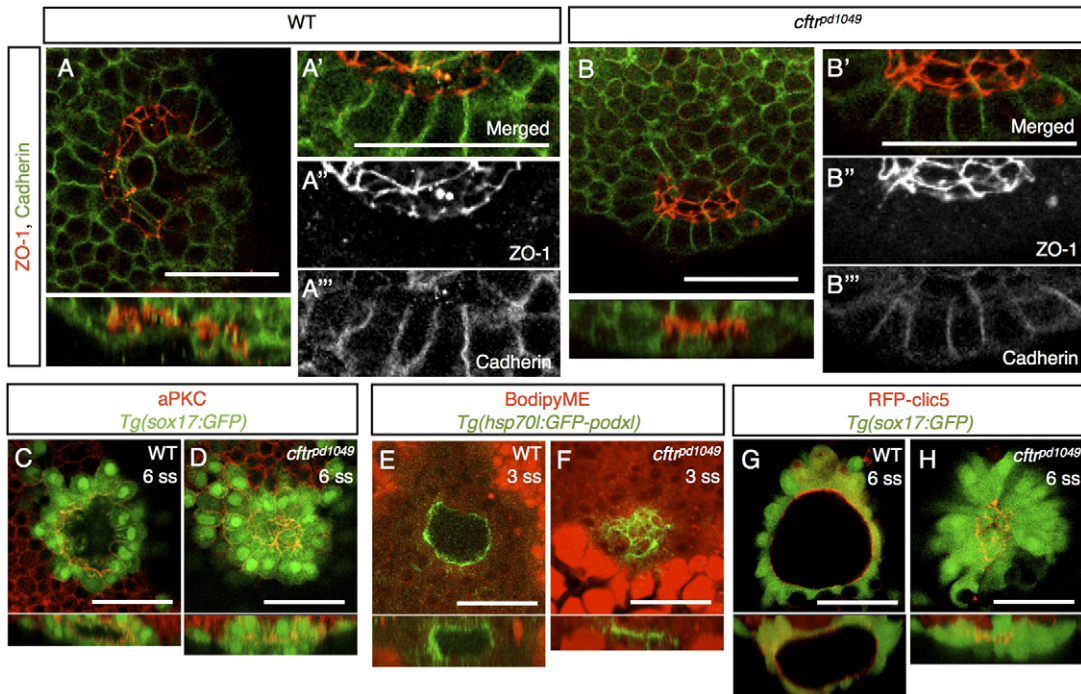


Fig. 4. Apical-basal polarity is not affected in *cfr^{pd1049}* mutants. (A,B) Confocal image and associated orthogonal projections of WT and *cfr^{pd1049}* mutant fish stained for ZO-1 and Cadherin. (A'-A''',B'-B''') Magnification of the KV epithelium to show localization of the polarity markers. (C,D) Confocal image and associated orthogonal projections of WT and *cfr^{pd1049}* mutant fish stained for aPKC and expressing *Tg(sox17:GFP)*. (E,F) Confocal image of WT and *cfr^{pd1049}* mutant KV expressing apically localized, GFP-tagged Podocalyxin. (G,H) Live confocal images of WT and *cfr^{pd1049}* mutant fish co-expressing an apical marker, RFP-Clic5b, and *Tg(sox17:GFP)*. Scale bars: 50 μm.

activation from 50% epiboly to 12 ss led to a 66% increase in the area of the KV lumen (Fig. 7A-C). We also tested whether the KV lumen could be reduced in size by inhibiting fluid secretion. The ion gradients driving Cfr-dependent fluid secretion are generated by the Na⁺/K⁺-ATPase. Treatment with low concentrations of ouabain, a potent and specific inhibitor of the Na⁺/K⁺-ATPase, from 50% epiboly to 10 ss decreased the area of the KV lumen by 33% (Fig. 7D-F). We further investigated the morphology of KV in fish treated with activators or inhibitors of fluid secretion using live confocal imaging and found that, although the lumen size was changed, the structure was otherwise organized properly, including the development of motile cilia (Fig. 7G-I).

We next tested whether Cfr function is required for fluid secretion specifically in KV by rescuing lumen expansion defects in several ways. We began by injecting WT and *cfr* mutant embryos with RNA encoding a Cfr-GFP fusion. Because we used the KV phenotype to distinguish mutant from WT embryos, we assayed KV rescue by examining the percentage of phenotypically mutant KV in whole clutches. A cross between parents heterozygous for *cfr^{pd1049}* resulted in a failure of KV lumen inflation in 25% of the clutch. Injection of *cfr-GFP* RNA at the one-cell stage reduced the proportion of the clutch that failed to undergo KV lumen expansion to ~10%, indicating that homozygous *cfr^{pd1049}* mutants were partially (~60%) rescued by RNA injection at the one-cell stage

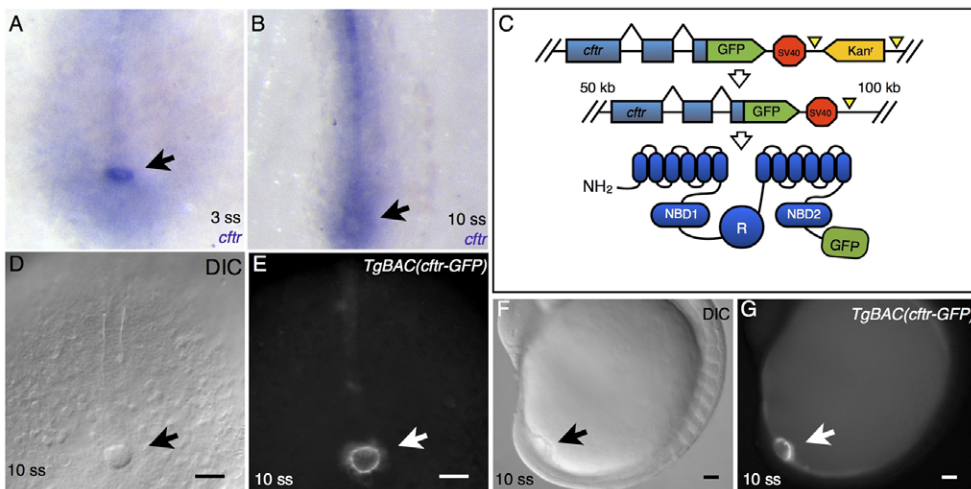


Fig. 5. *cfr* expression is enriched in KV. (A) At 3 ss, *in situ* hybridization detects *cfr* expression specifically in KV (arrow). (B) *In situ* hybridization showing *cfr* expression in KV (arrow) and the chordamesoderm in 10 ss embryos. (C) Schematic of the BAC recombineering procedure, showing the recombination target and the expected structure of the resulting GFP fusion protein. (D,F) DIC images showing ventral (D) and lateral (F) views of 10 ss embryos expressing *TgBAC(cfr-GFP)*. The arrow marks the characteristic KV structure. (E,G) Whole-mount epifluorescence of the embryos shown in D and F demonstrate specific KV expression of Cfr-GFP (arrows) at 10 ss. Scale bars: 50 μm.

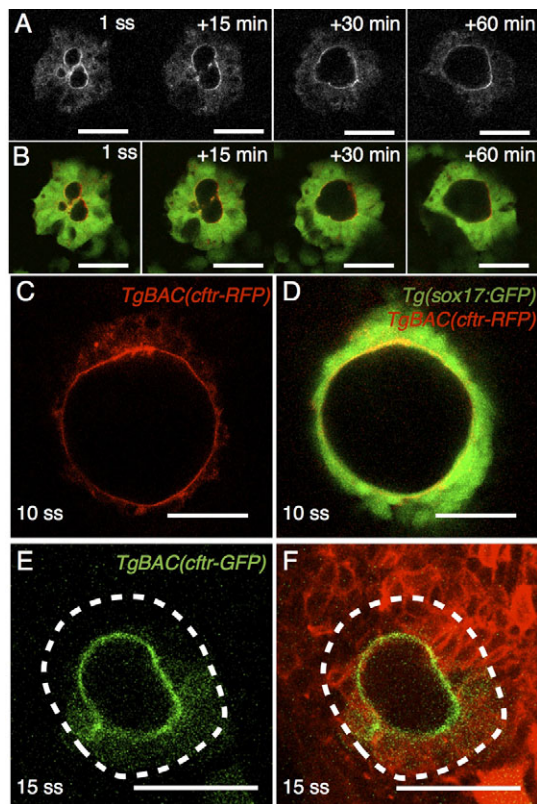


Fig. 6. Cfr is apically localized in KV epithelial cells throughout its morphogenesis. (A) Live, time-lapse confocal imaging of Cfr-RFP in *TgBAC(cfr-RFP); Tg(sox17:GFP)* embryos. Cfr-RFP is expressed and apically localized in KV throughout the initial stages of lumen coalescence. (B) Merge of the RFP and GFP channels. (C,D) Live confocal imaging of *TgBAC(cfr-RFP); Tg(sox17:GFP)* embryos at 10 ss shows that Cfr-RFP is localized apically in KV. (D) Merged view of Cfr-RFP and GFP. (E,F) Live confocal imaging of *TgBAC(cfr-GFP)* embryos injected with membrane-RFP RNA shows continued apical localization of Cfr-GFP until 15 ss. The dashed line marks the edge of KV. Scale bars: 50 μ m.

(Fig. 8A-D). The failure to completely rescue KV lumen expansion was probably due to mosaicism of the injected RNA (Carmany-Rampey and Moens, 2006). To test whether *cfr* is required in KV, we crossed *cfr^{pd1049}* mutants to the *TgBAC(cfr-GFP)* line, which is almost exclusively expressed in KV during lumen morphogenesis. This transgene was able to completely rescue lumen expansion, whereas non-expressing siblings maintained a 25% failure of KV lumen expansion ($n=289$) (Fig. 8E). Additionally, all *TgBAC(cfr-GFP)*-expressing fish had normal heart looping, indicating that the transgene was also able to rescue organ laterality. The *TgBAC(cfr-GFP)* rescue suggests that Cfr function is required specifically in KV and that the BAC transgene encodes a functional fusion protein.

We also attempted to phenocopy the *cfr^{pd1049}* KV phenotype by injecting a morpholino against Cfr (Bagnat et al., 2010) into DFCs (Amack and Yost, 2004). We found that DFC-specific injections were unable to prevent KV lumen expansion owing to mosaic uptake of the morpholino (Amack and Yost, 2004) (data not shown). This is not surprising given that fluid secretion is expected to function non-cell-autonomously.

Next, we determined whether forskolin and IBMX were acting through Cfr in KV by treating WT and *cfr^{pd1049}* mutants with these

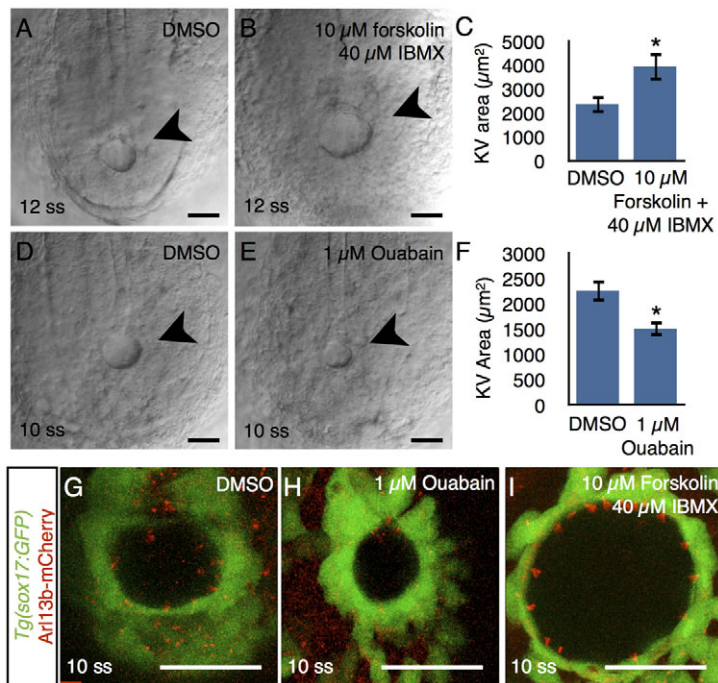
activators of fluid secretion. Forskolin and IBMX treatment failed to rescue KV lumen expansion in *cfr^{pd1049}* mutants, indicating that cAMP-stimulated fluid secretion acts through Cfr (Fig. 8F). Taken together, these studies demonstrate that in zebrafish, Cfr functions in KV to drive fluid secretion crucial for lumen expansion and morphogenesis of KV and LR patterning of the embryo.

DISCUSSION

Here, we describe a new role for Cfr in the regulation of fluid secretion necessary for KV morphogenesis and function. Live imaging of KV lumen morphogenesis showed several small lumens that coalesce into a single, central lumen. In the absence of Cfr activity, the KV lumen fails to inflate, indicating that fluid acts as a force driving lumen expansion and might also promote lumen coalescence. The zebrafish gut undergoes a similar process of *de novo* lumen formation, beginning with inflation of multiple small lumens, followed by their coalescence into one (Bagnat et al., 2007) and a similar role in *de novo* lumen formation and expansion has been shown for apical membrane or secreted mucins during tubulogenesis in the vertebrate vasculature (Strilić et al., 2010) and in the ommatidium (Husain et al., 2006) and hindgut (Syed et al., 2012) in *Drosophila*. The role of luminal content as a driving force during tube formation is most clearly exemplified by the *Drosophila* tracheal system, which becomes filled with a solid chitin matrix, then liquid and finally gas during its development (Tsarouhas et al., 2007). Altogether, these studies signify that the filling of the lumen is crucial for tubulogenesis in metazoans.

Although complete loss of Cfr function abrogated inflation of the KV lumen, it did not affect the specification, migration or the clustering of DFCs. Ciliogenesis has previously been shown to proceed coordinately with KV lumen expansion, raising the possibility of crosstalk between luminal volume and cilia length (Oteiza et al., 2010). Here, we found that in the absence of fluid secretion into the KV lumen, cilia morphogenesis and motility were unaffected, indicating that fluid secretion and flow are specified largely independently.

Although KV cilia length and number were unchanged in *cfr^{pd1049}* mutants, the absence of a KV lumen resulted in bilateral *spaw* expression. Previous research has demonstrated that bilateral *spaw* expression can be caused by defects in the midline barrier, which functions to prevent the diffusion of Spaw to the right side of the embryo (Long et al., 2003). In *cfr^{pd1049}* mutants, proper midline expression of *ntl* and *lefty1* indicate that midline integrity is not perturbed. Moreover, mutations that affect midline integrity result in heterotaxia, a phenotype rarely observed in *cfr^{pd1049}* mutants. This difference in organ situs in *cfr^{pd1049}* mutants can be explained by the fact that a majority of embryos with bilateral *spaw* expression did not show equivalent left and right *spaw*, but rather that expression on one side was more pronounced and extended anteriorly. Previous research in *Xenopus* has demonstrated that in embryos with bilateral *Nodal*, in which one side displays dominant expression, organ position is specified concordantly (Ohi and Wright, 2007). The remaining pool of *cfr^{pd1049}* embryos with equivalent left- and right-sided *spaw* expression might have been left-biased in a way *in situ* hybridization was not sensitive enough to detect. Similar patterns of bilateral *spaw* expression have also been observed upon loss of function of the Spaw antagonist Charon (Dand5 – Zebrafish Information Network), which also has no associated midline defect (Hashimoto et al., 2004). Although we are unable to completely rule out a contribution from the midline, our data strongly suggest that *cfr* is required specifically in KV for proper specification of organ laterality. However, the fact that we

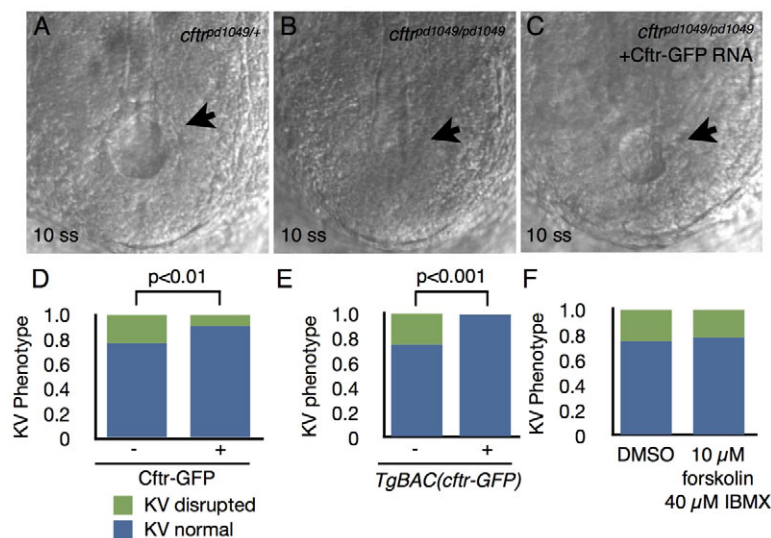


observe defects in organ laterality in only $\sim 30\%$ of *cftr*^{pd1049} mutants, instead of a complete randomization of laterality (50% penetrance), suggests that fluid flow in KV is not the only source of asymmetric information in the early zebrafish embryo. Consistent with this interpretation, previous studies in chicken, frog and zebrafish (Kawakami et al., 2005; Levin et al., 2002) suggested that KV might function to amplify earlier asymmetries, such as differences in H⁺/K⁺-ATPase activity and thus bias organ laterality in the absence of KV function.

Although our results demonstrate that *Cftr* plays an important role in the development of LR asymmetry in the zebrafish, it should be noted that organ laterality defects have not been observed in cystic fibrosis (CF) patients. This is probably due to morphological differences between the teleost KV and the laterality organs in other vertebrates. Whereas KV in zebrafish is an enclosed structure, the node in mammals and the gastrocoel roof plate in *Xenopus* are

indentations, where fluid may freely diffuse into the organ (Blum et al., 2007; Shook et al., 2004; Sulik et al., 1994). In fact, passing artificially generated fluid flow over the mouse node is sufficient to reverse organ laterality (Nonaka et al., 2002). It is also unknown whether *cftr* orthologs are expressed in the mouse node or frog gastrocoel roof plate. Further investigation will be required to determine whether embryonic fluid secretion is specifically required in the laterality organs of other vertebrates or if they utilize fluid secreted from other sources.

In CF patients, reduced fluid secretion leads to mucus buildup in the lungs, liver and pancreas, disrupting their function (Durie and Forstner, 1989; Gaskin et al., 1988; Matsui et al., 1998). The recent development of new animal models of CF will greatly improve understanding of the pathophysiology of CF (Rogers et al., 2008; Sun et al., 2010). Clinical data from patients and new animal models, such as the pig and the ferret, suggest that some defects



associated with CF might arise during development (Imrie et al., 1979; Olivier et al., 2012; Sturgess, 1984), a stage that remains difficult to access in these models with limited genetic tools. A developmentally accessible model will provide valuable insights into CFTR regulation and CF pathophysiology in various organs. The development of zebrafish *cftr* mutants provides an *in vivo* model in which to study human CFTR and assay drugs designed to correct the $\Delta F508$ -CFTR mutation and other pathologically relevant mutations. Future work may also shed light into the role Cftr plays in the development of the pancreas and other organs.

In summary, this study identifies a new role for Cftr in the regulation of fluid secretion into KV and for the development of LR asymmetry. It also highlights the importance of fluid secretion in lumen expansion during vertebrate morphogenesis. The relative simplicity and experimental accessibility of KV compared with other organs undergoing *de novo* lumen formation make KV an attractive model for studying fundamental mechanisms of lumen formation in vertebrates.

Acknowledgements

We thank Sean Ryan for help with cell culture experiments; members of the Bagnat lab for helpful discussions throughout this project; members of Ken Poss's lab for discussions and assistance with BAC recombineering; James Patton and Joshua Gamse for *in situ* hybridization probes; Brian Ciruna for an Ar113b-mCherry expression plasmid; Didier Stainier for providing the *Tg(sox17:GFP)* line; and Cagla Eroglu, Terry Lechler and Ken Poss for critical reading of this manuscript.

Funding

This work was funded by a National Institutes of Health (NIH) innovator grant [DP2OD006486 to M.B.]. Support for L.M. was provided by a NIH training grant [5T32HL098099-02]. Deposited in PMC for release after 12 months.

Competing interests statement

The authors declare no competing financial interests.

Supplementary material

Supplementary material available online at <http://dev.biologists.org/lookup/suppl/doi:10.1242/dev.091819/-/DC1>

References

- Amack, J. D. and Yost, H. J. (2004). The T box transcription factor no tail in ciliated cells controls zebrafish left-right asymmetry. *Curr. Biol.* **14**, 685-690.
- Amack, J. D., Wang, X. and Yost, H. J. (2007). Two T-box genes play independent and cooperative roles to regulate morphogenesis of ciliated Kupffer's vesicle in zebrafish. *Dev. Biol.* **310**, 196-210.
- Anderson, M. P., Gregory, R. J., Thompson, S., Souza, D. W., Paul, S., Mulligan, R. C., Smith, A. E. and Welsh, M. J. (1991). Demonstration that CFTR is a chloride channel by alteration of its anion selectivity. *Science* **253**, 202-205.
- Bagnat, M., Cheung, I. D., Mostov, K. E. and Stainier, D. Y. R. (2007). Genetic control of single lumen formation in the zebrafish gut. *Nat. Cell Biol.* **9**, 954-960.
- Bagnat, M., Navis, A., Herbreith, S., Brand-Arzamendi, K., Curado, S., Gabriel, S., Mostov, K. E., Huisken, J. and Stainier, D. Y. R. (2010). Cse11 is a negative regulator of CFTR-dependent fluid secretion. *Curr. Biol.* **20**, 1840-1845.
- Benharouga, M., Sharma, M., So, J., Haardt, M., Drzymala, L., Popov, M., Schwapach, B., Grinstein, S., Du, K. and Lukacs, G. L. (2003). The role of the C terminus and Na⁺/H⁺ exchanger regulatory factor in the functional expression of cystic fibrosis transmembrane conductance regulator in nonpolarized cells and epithelia. *J. Biol. Chem.* **278**, 22079-22089.
- Berger, H. A., Travis, S. M. and Welsh, M. J. (1993). Regulation of the cystic fibrosis transmembrane conductance regulator Cl⁻ channel by specific protein kinases and protein phosphatases. *J. Biol. Chem.* **268**, 2037-2047.
- Bisgrove, B. W., Essner, J. J. and Yost, H. J. (1999). Regulation of midline development by antagonism of lefty and nodal signaling. *Development* **126**, 3253-3262.
- Blum, M., Andre, P., Muders, K., Schweickert, A., Fischer, A., Bitzer, E., Bogusch, S., Beyer, T., van Straaten, H. W. M. and Viebahn, C. (2007). Ciliation and gene expression distinguish between node and posterior notochord in the mammalian embryo. *Differentiation* **75**, 133-146.
- Borovina, A., Superina, S., Voskas, D. and Ciruna, B. (2010). Vangl2 directs the posterior tilting and asymmetric localization of motile primary cilia. *Nat. Cell Biol.* **12**, 407-412.
- Brennan, J., Norris, D. P. and Robertson, E. J. (2002). Nodal activity in the node governs left-right asymmetry. *Genes Dev.* **16**, 2339-2344.
- Carmany-Rampey, A. and Moens, C. B. (2006). Modern mosaic analysis in the zebrafish. *Methods* **39**, 228-238.
- Cartwright, J. H. E., Piro, O. and Tuval, I. (2009). Fluid dynamics in developmental biology: moving fluids that shape ontogeny. *Hfspj* **3**, 77-93.
- Cermak, T., Doyle, E. L., Christian, M., Wang, L., Zhang, Y., Schmidt, C., Baller, J. A., Somia, N. V., Bogdanove, A. J. and Voytas, D. F. (2011). Efficient design and assembly of custom TALEN and other TAL effector-based constructs for DNA targeting. *Nucleic Acids Res.* **39**, e82.
- Doyle, E. L., Booher, N. J., Standage, D. S., Voytas, D. F., Brendel, V. P., Vandyk, J. K. and Bogdanove, A. J. (2012). TAL Effector-Nucleotide Targeter (TALEN) 2.0: tools for TAL effector design and target prediction. *Nucleic Acids Res.* **40**, W117-W122.
- Durie, P. R. and Forstner, G. G. (1989). Pathophysiology of the exocrine pancreas in cystic fibrosis. *J. R. Soc. Med.* **82** Suppl. **16**, 2-10.
- Essner, J. J., Amack, J. D., Nyholm, M. K., Harris, E. B. and Yost, H. J. (2005). Kupffer's vesicle is a ciliated organ of asymmetry in the zebrafish embryo that initiates left-right development of the brain, heart and gut. *Development* **132**, 1247-1260.
- Farooq, M., Sulochana, K. N., Pan, X., To, J., Sheng, D., Gong, Z. and Ge, R. (2008). Histone deacetylase 3 (hdac3) is specifically required for liver development in zebrafish. *Dev. Biol.* **317**, 336-353.
- Gaskin, K. J., Waters, D. L., Howman-Giles, R., de Silva, M., Earl, J. W., Martin, H. C., Kan, A. E., Brown, J. M. and Dorney, S. F. (1988). Liver disease and common-bile-duct stenosis in cystic fibrosis. *N. Engl. J. Med.* **318**, 340-346.
- Hashimoto, H., Rebagliati, M., Ahmad, N., Muraoka, O., Kurokawa, T., Hibi, M. and Suzuki, T. (2004). The Cerberus/Dan-family protein Charon is a negative regulator of Nodal signaling during left-right patterning in zebrafish. *Development* **131**, 1741-1753.
- Huang, P., Xiao, A., Zhou, M., Zhu, Z., Lin, S. and Zhang, B. (2011). Heritable gene targeting in zebrafish using customized TALENs. *Nat. Biotechnol.* **29**, 699-700.
- Husain, N., Pellikka, M., Hong, H., Klimentova, T., Choe, K.-M., Clandinin, T. R. and Tepass, U. (2006). The agrin/perlecan-related protein eyes shut is essential for epithelial lumen formation in the Drosophila retina. *Dev. Cell* **11**, 483-493.
- Imrie, J. R., Fagan, D. G. and Sturgess, J. M. (1979). Quantitative evaluation of the development of the exocrine pancreas in cystic fibrosis and control infants. *Am. J. Pathol.* **95**, 697-708.
- Kawakami, K. (2004). Transgenesis and gene trap methods in zebrafish by using the Tol2 transposable element. *Methods Cell Biol.* **77**, 201-222.
- Kawakami, Y., Raya, A., Raya, R. M., Rodríguez-Esteban, C. and Izpisua Belmonte, J.-C. (2005). Retinoic acid signalling links left-right asymmetric patterning and bilaterally symmetric somitogenesis in the zebrafish embryo. *Nature* **435**, 165-171.
- Kramer-Zucker, A. G., Olale, F., Haycraft, C. J., Yoder, B. K., Schier, A. F. and Drummond, I. A. (2005). Cilia-driven fluid flow in the zebrafish pronephros, brain and Kupffer's vesicle is required for normal organogenesis. *Development* **132**, 1907-1921.
- Kwan, K. M., Fujimoto, E., Grabher, C., Mangum, B. D., Hardy, M. E., Campbell, D. S., Parant, J. M., Yost, H. J., Kanki, J. P. and Chien, C.-B. (2007). The Tol2kit: a multisite gateway-based construction kit for Tol2 transposon transgenesis constructs. *Dev. Dyn.* **236**, 3088-3099.
- Lee, E. C., Yu, D., Martinez de Velasco, J., Tessarollo, L., Swing, D. A., Court, D. L., Jenkins, N. A. and Copeland, N. G. (2001). A highly efficient Escherichia coli-based chromosome engineering system adapted for recombinogenic targeting and subcloning of BAC DNA. *Genomics* **73**, 56-65.
- Levin, M., Thorlin, T., Robinson, K. R., Nogi, T. and Mercola, M. (2002). Asymmetries in H⁺/K⁺-ATPase and cell membrane potentials comprise a very early step in left-right patterning. *Cell* **111**, 77-89.
- Li, N., Wei, C., Olena, A. F. and Patton, J. G. (2011). Regulation of endoderm formation and left-right asymmetry by miR-92 during early zebrafish development. *Development* **138**, 1817-1826.
- Long, S., Ahmad, N. and Rebagliati, M. (2003). The zebrafish nodal-related gene southpaw is required for visceral and diencephalic left-right asymmetry. *Development* **130**, 2303-2316.
- Lowery, L. A. and Sive, H. (2005). Initial formation of zebrafish brain ventricles occurs independently of circulation and requires the *nagie oko* and *snakehead/atp1a1a.1* gene products. *Development* **132**, 2057-2067.
- Marjoram, L. and Wright, C. (2011). Rapid differential transport of Nodal and Lefty on sulfated proteoglycan-rich extracellular matrix regulates left-right asymmetry in Xenopus. *Development* **138**, 475-485.
- Matsui, H., Grubb, B. R., Tarran, R., Randell, S. H., Gatzky, J. T., Davis, C. W. and Boucher, R. C. (1998). Evidence for periciliary liquid layer depletion, not abnormal ion composition, in the pathogenesis of cystic fibrosis airways disease. *Cell* **95**, 1005-1015.
- McGrath, J., Somlo, S., Makova, S., Tian, X. and Brueckner, M. (2003). Two populations of node monocilia initiate left-right asymmetry in the mouse. *Cell* **114**, 61-73.

- Meder, D., Shevchenko, A., Simons, K. and Füllekrug, J. (2005). Gp135/podocalyxin and NHERF-2 participate in the formation of a preapical domain during polarization of MDCK cells. *J. Cell Biol.* **168**, 303-313.
- Miller, J. C., Tan, S., Qiao, G., Barlow, K. A., Wang, J., Xia, D. F., Meng, X., Paschon, D. E., Leung, E., Hinkley, S. J. et al. (2011). A TALE nuclease architecture for efficient genome editing. *Nat. Biotechnol.* **29**, 143-148.
- Moyer, J. H., Lee-Tischler, M. J., Kwon, H. Y., Schrick, J. J., Avner, E. D., Sweeney, W. E., Godfrey, V. L., Cacheiro, N. L., Wilkinson, J. E. and Woychik, R. P. (1994). Candidate gene associated with a mutation causing recessive polycystic kidney disease in mice. *Science* **264**, 1329-1333.
- Nauli, S. M., Alenghat, F. J., Luo, Y., Williams, E., Vassilev, P., Li, X., Elia, A. E. H., Lu, W., Brown, E. M., Quinn, S. J. et al. (2003). Polycystins 1 and 2 mediate mechanosensation in the primary cilium of kidney cells. *Nat. Genet.* **33**, 129-137.
- Nonaka, S., Shiratori, H., Saijoh, Y. and Hamada, H. (2002). Determination of left-right patterning of the mouse embryo by artificial nodal flow. *Nature* **418**, 96-99.
- Ohi, Y. and Wright, C. V. E. (2007). Anteriorward shifting of asymmetric Xnr1 expression and contralateral communication in left-right specification in *Xenopus*. *Dev. Biol.* **301**, 447-463.
- Olivier, A. K., Yi, Y., Sun, X., Sui, H., Liang, B., Hu, S., Xie, W., Fisher, J. T., Keiser, N. W., Lei, D. et al. (2012). Abnormal endocrine pancreas function at birth in cystic fibrosis ferrets. *J. Clin. Invest.* **122**, 3755-3768.
- Oteiza, P., Köppen, M., Concha, M. L. and Heisenberg, C.-P. (2008). Origin and shaping of the laterality organ in zebrafish. *Development* **135**, 2807-2813.
- Oteiza, P., Köppen, M., Krieg, M., Pulgar, E., Farias, C., Melo, C., Preibisch, S., Müller, D., Tada, M., Hartel, S. et al. (2010). Planar cell polarity signalling regulates cell adhesion properties in progenitors of the zebrafish laterality organ. *Development* **137**, 3459-3468.
- Riordan, J. R., Rommens, J. M., Kerem, B., Alon, N., Rozmahel, R., Grzelczak, Z., Zielenski, J., Lok, S., Plavsic, N., Chou, J. L. et al. (1989). Identification of the cystic fibrosis gene: cloning and characterization of complementary DNA. *Science* **245**, 1066-1073.
- Rogers, C. S., Stoltz, D. A., Meyerholz, D. K., Ostedgaard, L. S., Rokhlina, T., Taft, P. J., Rogan, M. P., Pezzulo, A. A., Karp, P. H., Itani, O. A. et al. (2008). Disruption of the CFTR gene produces a model of cystic fibrosis in newborn pigs. *Science* **321**, 1837-1841.
- Saijoh, Y., Oki, S., Ohishi, S. and Hamada, H. (2003). Left-right patterning of the mouse lateral plate requires nodal produced in the node. *Dev. Biol.* **256**, 160-172.
- Sakaguchi, T., Kikuchi, Y., Kuroiwa, A., Takeda, H. and Stainier, D. Y. R. (2006). The yolk syncytial layer regulates myocardial migration by influencing extracellular matrix assembly in zebrafish. *Development* **133**, 4063-4072.
- Sarmah, B., Latimer, A. J., Appel, B. and Wenthe, S. R. (2005). Inositol polyphosphates regulate zebrafish left-right asymmetry. *Dev. Cell* **9**, 133-145.
- Schweickert, A., Weber, T., Beyer, T., Vick, P., Bogusch, S., Feistel, K. and Blum, M. (2007). Cilia-driven leftward flow determines laterality in *Xenopus*. *Curr. Biol.* **17**, 60-66.
- Shook, D. R., Majer, C. and Keller, R. (2004). Pattern and morphogenesis of presumptive superficial mesoderm in two closely related species, *Xenopus laevis* and *Xenopus tropicalis*. *Dev. Biol.* **270**, 163-185.
- Snelson, C. D., Santhakumar, K., Halpern, M. E. and Gamse, J. T. (2008). Tbx2b is required for the development of the parapineal organ. *Development* **135**, 1693-1702.
- Strilić, B., Eglinger, J., Krieg, M., Zeeb, M., Axnick, J., Babál, P., Müller, D. J. and Lammert, E. (2010). Electrostatic cell-surface repulsion initiates lumen formation in developing blood vessels. *Curr. Biol.* **20**, 2003-2009.
- Sturgess, J. M. (1984). Structural and developmental abnormalities of the exocrine pancreas in cystic fibrosis. *J. Pediatr. Gastroenterol. Nutr.* **3 Suppl. 1**, S55-S66.
- Sulik, K., Dehart, D. B., Ilangaki, T., Carson, J. L., Vrablic, T., Gesteland, K. and Schoenwolf, G. C. (1994). Morphogenesis of the murine node and notochordal plate. *Dev. Dyn.* **201**, 260-278.
- Sun, Z., Amsterdam, A., Pazour, G. J., Cole, D. G., Miller, M. S. and Hopkins, N. (2004). A genetic screen in zebrafish identifies cilia genes as a principal cause of cystic kidney. *Development* **131**, 4085-4093.
- Sun, X., Sui, H., Fisher, J. T., Yan, Z., Liu, X., Cho, H.-J., Joo, N. S., Zhang, Y., Zhou, W., Yi, Y. et al. (2010). Disease phenotype of a ferret CFTR-knockout model of cystic fibrosis. *J. Clin. Invest.* **120**, 3149-3160.
- Suster, M. L., Sumiyama, K. and Kawakami, K. (2009). Transposon-mediated BAC transgenesis in zebrafish and mice. *BMC Genomics* **10**, 477.
- Syed, Z. A., Bougé, A.-L., Byri, S., Chavoshi, T. M., Täng, E., Bouhin, H., van Dijk-Härd, I. F. and Uv, A. (2012). A luminal glycoprotein drives dose-dependent diameter expansion of the *Drosophila melanogaster* hindgut tube. *PLoS Genet.* **8**, e1002850.
- Tsarouhas, V., Senti, K.-A., Jayaram, S. A., Tiklová, K., Hemphälä, J., Adler, J. and Samakovlis, C. (2007). Sequential pulses of apical epithelial secretion and endocytosis drive airway maturation in *Drosophila*. *Dev. Cell* **13**, 214-225.
- Westerfield, M. (2000). *The Zebrafish Book. A Guide for the Laboratory Use of Zebrafish (Danio rerio)*. Eugene, OR: University of Oregon Press.
- Wilson, S. M., Olver, R. E. and Walters, D. V. (2007). Developmental regulation of luminal lung fluid and electrolyte transport. *Respir. Physiol. Neurobiol.* **159**, 247-255.
- Yelon, D., Horne, S. A. and Stainier, D. Y. R. (1999). Restricted expression of cardiac myosin genes reveals regulated aspects of heart tube assembly in zebrafish. *Dev. Biol.* **214**, 23-37.
- Zaghloul, N. A. and Katsanis, N. (2011). Zebrafish assays of ciliopathies. *Methods Cell Biol.* **105**, 257-272.